

# THEORY OF THE EM DRIVE IN TM MODE BASED ON MACH-LORENTZ THEORY

Jean-Philippe Montillet  
*Ecole Polytechnique Fédérale*  
*Lausanne, Switzerland*

Various theories have recently emerged to explain the anomalous thrust generated by the controversial EM Drive [1,2]. This work proposes a model based on the theory of the Mach-Lorentz thruster [3]. The thrust is generated by the combination between the Lorentz force and the Woodward effect [4]. The development has been facilitated due the discussions with Dr. José Rodal and Prof. Heidi Fearn. In addition, our approach is only based on the results from the experiments in TM mode released by the NASA Eagleworks group [5,6]. The purpose of this communication is to improve our model using feedback from scientists and to some extends with the EM Drive community in order to point out weaknesses on some of our assumptions and to plan future campaigns of experimental tests.

## 1. OVERVIEW

Since the first experiment at the beginning of this new millennium, the EM Drive has been the focus of many critics from scientists and engineers. In addition, public debates have also contributed in casting doubts on this possible technology. However, the latest tests and measurements by various academics [7] and government agencies [5], which should have dismissed this technology once and for all, have confirmed the anomalous thrust generated by this device. This latest development has sparked new interests for this device, which could play a critical role in space exploration of our solar system [8]. Nevertheless, the ultimate goal remains the creation of a model of the EM Drive supporting the experiments.

In the last two decades, various theories have emerged to understand the thrust generated by the EM Drive. The author in [1] or [2] developed a theory based on the difference of radiation pressure forces on the end plates of the cavity. More recently, an explanation of the anomalous thrust has been supported by the introduction of the Unruh radiation [9]. Another theory [10] attempts to model this exotic propulsion engine based on the emission of paired photons expelled through the cavity end walls and generating the recorded thrust. In [11], the thrust is the result of a man-made gravitational field gradient taking place inside the cavity. Other emerging theories can be found online. Among all those theories, we are here only interested in the application of the theory of the Mach-Lorentz thruster (MLT) [3] to the EM Drive. Note that the MLT is also called Mach Effect Gravitational Assist-drive (MEGA-drive). This theory is based on the Lorentz force coupled to the Woodward effect [12] in order to explain the anomalous thrust. The Woodward effect relies on the Mach's principle, which defines inertia within general relativity theory [13], and demonstrates that inertia is caused by the gravitational interaction between an object and massive bodies in the distant universe. The Woodward effect describes a way to extract a linear force from an accelerating object which is undergoing internal deformation and mass-energy fluctuations. Momentum is conserved via the gravitational field. Experiments with capacitors and piezoelectric materials have reproduced the Woodward effect in laboratory environment [4].

Our model assumes that each element constituting the EM cavity (frustum), namely the two end plates and the conical wall, responds independently to the EM waves propagating inside the cavity and reflected on the walls. Each element is modelled with a capacitor in series with a resistance and in parallel with an inductor. The capacitor models the EM excitation phenomenon from the waves reflecting on the end plates in TM modes. Thus, the assumptions are from the EM excitation: creating surface currents on the surface of the walls; generating an EM energy density "stored" in the skin layer of the copper end plates (e.g., evanescent waves [14]). The capacitor charges and discharges instantaneously due to the creation and dissipation of the charges. If the capacitor is related to the EM excitation mostly due to the electric field, the inductor is then modelling the EM excitation with the magnetic field via the Eddy (Foucault) currents phenomenon [15]. The Eddy currents are loops of electrical currents induced within conductors by a changing magnetic field in the conductor, hence generated when the vector field and the cavity walls are intersecting. While the capacitor and inductor model two different phenomena, the additional strong assumption is that the capacitor should be the dominant effect when the electric field is perpendicular to the wall. However, if the electric field is parallel to the wall or if something prevents the EM excitation on the wall, the inductor should then be the dominant model. For example, when inserting some dielectric (e.g., High-density polyethylene (HDPE)) to one end (e.g., small end plate), it could prevent (partially) the creation of electric charges on this particular

wall. The electric field is more attenuated than the magnetic field when passing through the dielectric field (i.e. electrical insulator properties [16]). Thus, we model this phenomenon by increasing the resistance in series with the capacitor.

Now, the current propagating at the interior surface of the conical wall (between the two end plates) is also going through the magnetic field generated inside the cavity, hence resulting in a Lorentz force. This force is the result of the integration on the whole interior surface. However, this force alone cannot be responsible for any movement of the cavity due to the conservation of momentum as explained further in this document.

Secondly, the MLT model is based on the assumption that the Woodward effect is generating the thrust and it is triggered by the Lorentz force. The variation of mass described in [4] is driven by the variation of EM energy density in the skin layer of the copper wall. Thus, the assumption is that the Woodward effect mostly relies on the capacitor model of the cavity wall.

The next sections describe the various steps of this model based on the TM010 simulations and experiments [6, 22, 27]. It is worth emphasizing that for TM010 we use the cylinder terminology for this mode shape since there is no universal convention for mode shape terminology for a truncated cone. Notice that for a truncated cone the electromagnetic field in the axial direction is not constant.

In order to facilitate the understanding of the overall model, an analogy between electrical circuits and Newtonian mechanics is made. We must state clearly that there are two different mechanisms which can be modelled with an *RLC* circuit in this work. The first mechanism is the response to the EM excitation of each element composing the cavity which basically explains two phenomena described above: Eddy currents from the magnetic field, and the surface current from the electric field. The second analogy with the *RLC* circuit is used to explain the anomalous thrust by modelling the whole cavity. This model is fully developed in the following sections. However, our analogy does not relate to the well-known model of a specific EM cavity with an *RLC* circuit used in the analysis of the EM properties. Readers interested in this analogy can refer to [17].

## 2. SOME EQUATIONS AND DISCUSSIONS

### 2.1 Modelisation of the Three Steps: Electro-mechanics and Gravitational Coupling (EMG)

#### *RC circuit*

Let us first assume that there is no force or no thrust acting on the cavity. The electric field is exciting the end plates, and parallel to the conical wall (e.g., [18] or [19]). The capacitor models the EM excitation via the electric field on the end plates. Thus, the capacitor charges and discharges instantaneously due to the creation and dissipation of the charges by EM excitation on the surface of the end plates. The EM cavity can then be modelled as two capacitors in series charging/discharging instantaneously. Taking into account the dissipation intrinsic to the conductor properties, the cavity can be modelled such as a *RC* circuit. The equations read:

$$\begin{aligned} Ri + \frac{q}{C} &= 0 \\ R\partial_t q + \frac{q}{C} &= 0 \\ q(t) &\sim q_0 \exp\left(-\frac{t}{RC}\right) \end{aligned} \tag{1}$$

$q_0$  is the charge at  $t = 0$ . The equation of the charge  $q(t)$  shows that the dissipation of the initial charge  $q_0$  during the discharge time  $\tau = RC$ . That is why we can understand it such as a *switch on- switch off* of the capacitor. To evaluate the discharge time  $\tau$ , one can write the conservation of charge equation at the surface of the plates.

Let us consider the density of the charge  $\rho(t)$ , the conductivity of the copper  $\sigma$  and its permittivity  $\epsilon_r$ ,

then [14],

$$\begin{aligned}
\partial_t \rho(t) + \text{div} \vec{j} &= 0 \\
\partial_t \epsilon_r \epsilon_0 \vec{E} + \text{div} \sigma \vec{E} &= 0 \\
\epsilon_r \epsilon_0 \partial_t \Delta V + \sigma \Delta V &= 0 \\
V(t) &\sim V_0 \exp\left(-\frac{\sigma}{\epsilon_r \epsilon_0} t\right)
\end{aligned} \tag{2}$$

The discharge time  $\tau$  equal  $\frac{\epsilon_r \epsilon_0}{\sigma}$  or  $6 * 8.85e - 12 / 5.85e7 \sim 1e - 18$ s (values from [20]). Note that we assume at the surface of the plate  $\vec{E} = -\vec{\nabla}V$  (no magnetic potential).  $V_0$  is the potential at  $t = 0$  before the discharge. Now in order to evaluate the potential over the whole copper end plate, we integrate on the whole surface  $S$ . The difference of potential between the two end plates (without dielectric or HDPE insert) is then  $DV = (S_1 - S_2)V_0 \exp\left(-\frac{\sigma}{\epsilon_r \epsilon_0} t\right)$ . Within the frustum model,  $S$  is equal to  $\pi r^2$  ( $r$  the radius of the end plate). With the insertion of the HDPE (or dielectric) on the end with surface  $S_2$ , the difference of potential is then equal to  $DV \sim S_1 V_0 \exp\left(-\frac{\sigma}{\epsilon_r \epsilon_0} t\right)$ . Now, the Eddy currents generated on the conical wall due to the perpendicular magnetic field, compete with the current propagating from the difference of electric potential between the end plates (from large to small end plate). The direction of the Eddy currents depends on  $\text{curl} \vec{B}$  (see the Maxwell equation  $\text{curl} \vec{B} = \mu_0 \vec{j}$ , with  $\mu_0$  the permeability of the vacuum and  $\vec{j}$  the Eddy currents). The two currents propagate in opposite directions in the TM010 scenario. In addition, the Eddy currents may have a larger amplitude than the other current propagating on the conical wall.

In the first step, **the main assumption is the creation of charges at the surface of the end plates** in TM mode.

#### *The acceleration of the cavity due to the Lorentz force*

The second step is when a force is generated acting on the cavity. The current propagates inside the magnetic field, and thus triggering a Lorentz force  $F_{Lo}$ . As previously said, this current can be either the Eddy current or the current induced by the difference of electrical potential between the two end plates. Let us assume that an alternative current (AC) is propagating between the two end plates. In terms of circuit analogy, the cavity is now a *RLC* circuit with an induced electromotive force  $\varepsilon$ :

$$Ri + \frac{q}{C} + L\partial_t i - \varepsilon = 0 \tag{3}$$

$L\partial_t i$  is equivalent to the mechanical action of the cavity getting accelerated (or  $m\partial_t v$  in classical mechanics (Newton's second law),  $m$  the mass of the cavity and  $v$  the speed).  $\varepsilon$  can be expressed such as  $\varepsilon = -\partial_t \phi_B(t)$ , with  $\phi_B(t)$  the magnetic flux through the copper conical wall surface [14]. In classical mechanics (i.e. Newton second law), when projecting the forces on the Z-axis ( see Figure 1 ), the equation (3) becomes:

$$m\partial_t^2 z = \alpha\partial_t z - Kz + F_{Lo} \tag{4}$$

where  $\alpha\partial_t z$  is the dissipative force due to the resistivity of the copper when the current propagates. Note that the force due to the weight of the cavity is perpendicular to the axis onto we project the forces and the Z-axis direction is toward the small end plate.

Let us estimate the Lorentz force applied to one electron (with charge  $q_e$  and speed  $v_e$ ) moving through the magnetic field  $\vec{B}$  at the surface of the conical wall

$$\vec{F}_{Lo} = q_e v_e \times \vec{B}$$

$\times$  is the vectorial product. Using the convention in [18] and [19], the magnetic field is parallel to the conical wall with only a component on the surface of the azimuth direction  $\vec{B} = B_\phi u_\phi$ . The apex angle of the frustum is defined as  $2\theta_w$ . The expression of the force on the Z-axis is then  $\vec{F}_{Lo}$ :

$$\vec{F}_{Lo} = q_e v_e B_\phi \sin(\theta_w) u_z$$

The displacement of the electrons is collinear to the unit length  $\vec{dl}$  of the conical wall. If we assume that the number density of electrons in copper is  $n_{Cu}$ ,  $dS$  the unit surface, then we can estimate the force over  $dl$

$$\vec{F}_{Lo} = n_{Cu} v_e dS dl B_\phi \sin(\theta_w) u_z$$

Let us assume the current with an amplitude  $dI_0 = n_{Cu} v_e dS$ . Then the Lorentz force per unit of length  $dl$  is:

$$\vec{F}_{Lo} = dI_0 dl B_\phi \sin(\theta_w) u_z \quad (5)$$

Using the axis as defined in Figure (and the same as in [19]), (5) becomes:

$$\vec{F}_{Lo} = dI_0 B_0 \exp(j(\omega t - Kz)) \cos(\theta_w) \sin(\theta_w) dz u_z \quad (6)$$

Note that the amplitude of the magnetic field at the surface of the conical wall is not constant and depends on the TM mode. In TM010, the experiments carried out by the NASA Eagleworks group,  $B_0$  is constant in azimuthal plane [6, 27], but not on the  $Z$ -axis. Thus, the Lorentz force can vary while the current propagates from one end to the other.

$dI_0$  can be integrated over the whole azimuth plane, but there is an assumption to be made: do we consider the current propagating over the whole thickness of the copper sheet, or just over an elementary part of it? It is important to underline that we are here using a simple model of the Lorentz force applied to free charges in a conductor. However, because surface charges are distributed over some infinitesimal depth, and those charges at greater depths are shielded by the others and therefore see a smaller electric field  $\vec{E}$ . In other words, the electric field created by the displacement of those charges decreases in amplitude with the depth in the conductor. Moreover, we did not take into account the possible effect of Kelvin polarization forces [21]. Note that (4) is only stated for a pedagogical point of view, because a creation of thrust from this equation is prevented by the momentum conservation principle (i.e. special relativity).

In the second step, the main assumption is the **current propagating at the surface of the conical wall** inside the cavity, hence generating the Lorentz Force.

#### *Generating the thrust*

The last step is the triggering of the Woodward effect generating the thrust. Basically, it is the introduction of  $\partial_t z \partial_t m$  into equation (4). As previously mentioned, the variation of mass of the cavity is due to the Woodward effect applied to the EM energy density *stored* in the skin layer of the copper end plate(s). Thus, the Woodward effect is mostly associated with the capacitor model and not the inductor for each element of the cavity, hence introducing a dielectric should reduce it. In TM010 mode, the effect should take place mostly on the end plates. Recalling the Woodward effect takes place only if the cavity is accelerated while the energy inside the cavity is fluctuating [4]. The variation of mass is translated into the equation [4],

$$\delta\rho_0(t) = \frac{1}{4\pi G} \left[ \frac{1}{\rho_0 c^2} \partial_t^2 U_0 - \left( \frac{1}{\rho_0 c^2} \right)^2 (\partial_t U_0)^2 \right] \quad (7)$$

$U_0$  is the energy of the system,  $\rho_0$  is the transient mass source, and  $c$  speed of light. Considering a rest energy  $\mathcal{E}$ , energy of the frustum at rest, including all the particles within the frustum with no EM excitation, one can state the famous Einstein's relationship in special relativity between  $\mathcal{E}$  and the rest mass  $\rho$ ,  $E = \rho c^2$ . In Appendix III, we justify the assumption that the variation with time of  $\mathcal{E}$  equal the variation of EM energy density with the capacitor model. The variation of EM energy in the copper end plate (skin layer) is expressed with  $du$  ( see Appendix I,(19)). The Woodward effect in (7) can then be rewritten

$$\delta\rho(t) = \frac{1}{4\pi G} \left[ \frac{1}{\rho c^2} \partial_t^2 u - \left( \frac{1}{\rho c^2} \right)^2 (\partial_t u)^2 \right] \quad (8)$$

The author in [4] calls  $\partial_t^2 U_0$  the impulse engine, and  $(\partial_t U_0)^2$  the wormhole. In the next section, we discuss the quantities  $\partial_t^2 u$  and  $\partial_t u$  and possible explanations in terms of EM theory. Note that the reader can find the rigorous derivation of (8) (based on [4]) with the assumptions of replacing the input power with the electromagnetic energy density in the appendices.

Finally, we assume that the Woodward effect creates a variation of mass (mass density) independently for each end plate when considering  $\mathcal{E}$  as the rest energy for one end plate in order to obtain (8). Let us then define:

- $\partial_t \rho L$  : variation of mass at large end plate
- $\partial_t \rho S$  : variation of mass at small end plate

with  $\partial_t m = \partial_t \rho L - \partial_t \rho S$ . (4) becomes

$$m \partial_t^2 z + \partial_t z (\partial_t \rho L - \partial_t \rho S) = \alpha \partial_t z - Kz + F_{Lo} \quad (9)$$

One needs to underline that the terms  $\alpha \partial_t z$  and  $Kz$  are intrinsic to the cavity parameters (i.e. resistivity, dimension), whereas the thrust or acceleration of the cavity ( $m \partial_t^2 z$ ) depends on the Lorentz force  $F_{Lo}$  and the relativistic terms coming from the Woodward effect  $\partial_t z (\partial_t \rho L - \partial_t \rho S)$ . One can underline that  $\partial_t \rho L - \partial_t \rho S$  can be interpreted as the Woodward effect created independently on each end plate with opposite direction (towards the outside of the cavity). Finally, the measurable thrust in the MLT comes from (9) which results from the coupling between the Lorentz force and the Woodward effect. Note that (9) sums up our model of the MLT.

In the last step, we assume that the **Lorentz force triggers the Woodward effect in order to generate the anomalous thrust.**

## 2.2 Variation of electromagnetic energy density

This section looks at numerical estimation of the EM energy density in the skin layer of the copper end plates.

### *Evanescent Waves in Copper Walls and Numerical Estimation*

As seen in the previous section, the surface surcharges disappeared as soon as they are created (with  $\vec{j} = \sigma_{Cu} \vec{E}$  and charge conservation equation, we have  $\tau_{relax} = \frac{\epsilon_0}{\sigma_{Cu}} \sim 10^{-18} \text{ s} \sim 0$ ). Note that in the following  $\epsilon = \epsilon_r \epsilon_0$  and  $\mu = \mu_r \mu_0$  as previously defined. We can then state the Maxwell equations at the surface of the copper wall end plates,

$$\left. \begin{aligned} \text{div} \vec{E}_{tot} &\sim 0, \\ \text{curl} \vec{E}_{tot} &= -\partial_t \vec{B}_{tot}, \\ \text{div} \vec{B}_{tot} &= 0, \\ \text{curl} \vec{B}_{tot} &= \mu \epsilon \partial_t \vec{E}_{tot} + \mu \sigma_{Cu} \vec{E}_{tot}, \end{aligned} \right\}$$

The wave equation is then [14]:

$$\Delta \vec{E}_{tot} = \mu \epsilon \partial_t^2 \vec{E}_{tot} + \mu \sigma_{Cu} \partial_t \vec{E}_{tot} \quad (10)$$

Assuming that the solution is a planar wave of the type  $\vec{E} = \vec{E}_0 e^{i(\omega t - \vec{k} \cdot \vec{r})}$  ( $i = \sqrt{-1}$ ), and knowing that on the end plates the electric field is only a radial component in TM mode (see [19]), then  $\vec{E}_0 = E_0 e^{i(\omega t - k r \cos \theta)} \vec{u}_r$  in spherical coordinates. One should expect by replacing it in the wave equation (10), the equation for the wavelength [14]

$$\begin{aligned} k^2 &= \mu \epsilon \omega^2 - i \mu \sigma_{Cu} \omega \\ k^2 &= \mu \epsilon \omega^2 \left(1 - i \frac{\sigma_{Cu}}{\omega \epsilon}\right) \end{aligned} \quad (11)$$

In the good conductors such as copper, one can make the assumption [14] that  $\frac{\sigma_{Cu}}{\omega \epsilon_0} \gg 1$ . Thus, (11) becomes

$$\begin{aligned} k^2 &= \mu \omega (-i \sigma_{Cu}) \\ k &= (1 - i) \sqrt{\frac{\sigma_{Cu} \mu \omega}{2}} \end{aligned} \quad (12)$$

Which ends up in an evanescent wave taking into account the real ( $k_1$ ) and imaginary part ( $k_2$ ) of the wavelength,  $\vec{E} = E_0 e^{-k_1 r \cos \theta} e^{i(\omega t - k_2 r \cos \theta)} \vec{u}_r$ . Now, we can estimate the energy density of the EM field

$\langle w \rangle = \langle u_E \rangle + \langle u_B \rangle$  with

$$\begin{aligned}
\langle u_E \rangle &= \frac{\epsilon C u}{2\pi} \int_0^{2\pi} \text{Re}\{E \cdot E^*\} dt \\
\langle u_E \rangle &= \frac{\epsilon_0}{2\pi} \int_0^{n\tau_r} \text{Re}\{E \cdot E^*\} dt \\
\langle u_E \rangle &= \frac{\epsilon_0}{2\pi} \int_0^{n\tau_r} E_0^2 e^{-2k_1 r} \cos^2(\omega t - k_2 r \cos\theta) dt \\
\langle u_E \rangle &\sim \frac{n\tau_r \epsilon_0}{2\pi} E_0^2 e^{-2k_1 r \cos\theta}
\end{aligned} \tag{13}$$

we assume that the Evanescent waves are created by the surface charges only during the relaxation time as explained above.  $\tau_r$  is part of relaxation time  $\tau_{rel}$  when the charges create the surface current. In the  $2\pi$  average interval, there is  $n\tau_r$  ( $n\tau_r \ll 1$ ). In the remaining time we consider the integral null. The first derivative of the EM energy density for the electric field is

$$\begin{aligned}
\langle \partial_t u_E \rangle &= \frac{\epsilon_0}{2\pi} \int_0^{2\pi} \text{Re}\{2E \cdot \partial_t E^*\} dt \\
\langle \partial_t u_E \rangle &= \frac{\epsilon_0 2\omega}{2\pi} \int_0^{n\tau_{rel}} E_0^2 e^{-2k_1 r} \sin(\omega t - k_2 r) \cos(\omega t - k_2 r) dt \\
\langle \partial_t u_E \rangle &\sim \frac{n\tau_{rel} \omega \epsilon_0}{2\pi} E_0^2 e^{-2k_1 r} \\
\langle \partial_t u_E \rangle &\sim \omega \langle u_E \rangle
\end{aligned} \tag{14}$$

The same development can be applied to the second derivative

$$\begin{aligned}
\langle \partial_t^2 u_E \rangle &\sim 2\omega \langle \partial_t u_E \rangle \\
\langle \partial_t^2 u_E \rangle &\sim \frac{n\tau_{rel} 2\omega^2 \epsilon_0}{2\pi} E_0^2 e^{-2k_1 r}
\end{aligned} \tag{15}$$

For the magnetic field, one can estimate with  $\text{curl} \vec{E} = -\partial_t \vec{B}$ . Choosing a spherical coordinates referential (Figure),

$$\begin{aligned}
\text{curl} \vec{E} &= \frac{-1}{r} \partial_\theta E \vec{u}_\phi \\
&= -i\omega \vec{B} \\
\vec{B} &= \left( \frac{k_1 \sin\theta}{\omega} (1-i) \right) E \vec{u}_\phi
\end{aligned} \tag{16}$$

In the same way we estimated  $\langle u_E \rangle$ , one can estimate the magnetic energy density

$$\begin{aligned}
\langle u_B \rangle &= \frac{1}{\mu 2\pi} \int_0^{n\tau_{rel}} \text{Re}\{B \cdot B^*\} dt \\
\langle u_B \rangle &\sim \frac{1}{\mu \pi} \left( \frac{k_1 \sin\theta}{\omega} \right)^2 E_0^2 e^{-2k_1 r \cos\theta} n\tau_{rel} \\
\langle \partial_t u_B \rangle &\sim \omega \langle u_B \rangle \\
\langle \partial_t^2 u_B \rangle &\sim 2\omega^2 \langle u_B \rangle
\end{aligned} \tag{17}$$

However,

$$\begin{aligned}
\frac{\langle u_E \rangle}{\langle u_B \rangle} &\sim \frac{\epsilon}{\mu} \frac{\omega^2}{k_1^2 \sin^2\theta} \\
&\sim \frac{2\epsilon\omega}{\mu^2 \sigma C u} \gg 1
\end{aligned} \tag{18}$$

Because  $\frac{\langle u_E \rangle}{\langle u_B \rangle} \gg 1$ , the energy density of the EM field is mainly the contribution from the electric field. Finally, additional measurements on  $n$  can check the assumption on the order of magnitude of the EM energy density.

In this section, simulations of the copper frustum in TM010 mode has been performed by Christian Ziep using FEKO software [28]. The frustum is model as described in [22] and [27] without a dielectric insert. It is orientated following the Z-axis with the direction pointing towards the small end plate. The dimension of the cavity follows: 228.6 mm (height), 158.75 mm (diameter small end plate), 279.65 mm (diameter big end plate). The antenna model is an electrical dipole placed in the middle of the cavity. The input power is equal to 1W (30 dBm) with central frequency 0.9598 GHz and quality factor  $Q$  equal to 20.38. The resonant frequency is then estimated at 1020 MHz. Figure 2(A) displays the magnetic field inside the cavity perpendicular to the conical wall and parallel to the end plates as described in [18] and [19]. Figure 2(B) displays the electric field perpendicular to the end plates.

Now, the surface currents on the cavity walls are simulated following the previous description. Figure 3 (A,B) display the amplitude of the electric (E) and magnetic fields (H) at the surface of the conical wall as a function of the height; Figure 3 (C,D) the amplitude of the E and H-field at the surface of the small end plate; and Figure 3 (E,F) the amplitude of the E and H fields at the surface of the large end plate. The results show that the amplitude of the currents at the surface of the conical wall follows a gradient decreasing with the increase of the height of the frustum. It is in agreement with the observations that both E and H fields are larger (on average) at the surface of the large end than at the small end. Thus, the gradient of the amplitude of the wall current accommodates with the amplitude of simulated E and H fields at the surface of the end plates.

One assumption in our MLT model is the current propagating from large to small end plate due to the difference of electrical potential. In the simulations, the current at the surface of the conical wall propagates towards the large end plate. Thus, it seems that those currents are Eddy currents generated by the H field. As previously underlined, the Eddy currents could have higher amplitude than the one due to difference of electrical potential. This result underlines this phenomenon. In addition, the electric field at the surface of the large end plate is higher than at the small end plate, which supports a greater EM excitation. Based on our assumption that the Woodward effect is directly related to the skin depth effect taking place on the cavity wall, this effect should then be greater on the large end than on the small end. It has been shown in [6] that, in this experiment, the anomalous thrust is towards the large end plate. This result is in agreement with (9), assuming that the Woodward effect displaces the cavity towards the large end due to  $\delta\rho_L > \delta\rho_S$ . However, further study is required to understand the role of the Lorentz force taking place on the conical wall in the amplitude of the anomalous thrust.

### 3. CONCLUDING REMARKS

This model was based on a few results on the TM010 mode (i.e. [5,6, 22, 27]) and preliminary simulations. The study takes into account the EM excitation of each element of the cavity resulting in modelling them with a capacitor with a resistance in series, and an inductor in parallel. Thus, two types of currents are then taking into account: Eddy currents from transverse magnetic field and surface currents from electric field excitation. It is then produced a surface currents ( $dI_0$ ) on the conical wall, hence creating a Lorentz force. The last step of our model is the generation of thrust using the Woodward effect. However, the thrust is only produced by a coupling between the Lorentz force and the Woodward effect from (9) in order to guarantee momentum conservation principle. Only a careful analysis via simulations and experiments of the frustum for a specific mode can quantify the contribution of those currents to the proposed model of the thrust.

The proposed model is just at an early development stage where many assumptions must be validated. For example, the theory stands at the moment with those few points to check:

- Estimation of the currents on the cavity walls due to the electric and magnetic fields.
- On the need to estimate the AC current  $I_0$  on the conical wall and the Lorentz force  $\vec{F}_{Lo}$  through simulations and experiments with different scenarios (e.g., with and without HDPE).
- Better understanding of the coupling between the acceleration of the cavity due to  $\vec{F}_{Lo}$  and the Woodward effect.
- The variation of mass  $\delta\rho(t)$  in (8) with the first and second derivatives of the EM energy density.

Overall, our assumptions on this model have to be compared with the results from following experimentations. One can underline

- The model can be invalidated if there is still a non negligible thrust if we use superconductive materials for the frustum in order to eliminate (or reduce drastically) all skin depth effects on the cavity walls (suggested by Prof. J. Woodward).
- The first and second steps of this model rely on standard EM theory. One needs to estimate the average electric field at the surface of the end plates in order to get some measurements for the amplitude of the difference of electric potential (DV) and also to confirm the simulations.

Furthermore, at the time of writing this manuscript, NASA Eagleworks laboratory has released a full study supporting the EM Drive generating a thrust in TM mode [5,6]. New experiments are planned to test the TE mode, which can help supporting or not this model. We also acknowledge that some engineers have recently carried out tests involving various new designs of the EM Drive showing successfully an anomalous thrust. The TE mode is the next step in order to produce a complete MLT model of the EM Drive and its anomalous thrust. To conclude, this new engine can be an example of EMG coupling if the presented model is validated.

#### 4. Acknowledgements

The author would like to acknowledge the great contribution to this article by Christian Ziep, who conducted several numerical analyses of the EM Drive truncated cone cavity using FEKO software; some of those results are reproduced in this article. Also acknowledged are the contributions of people involved in developing the presented model via discussions with the author, including Paul March (NASA, Eagleworks) and Todd J. Desiato (Warp Drive Tech.).

#### Addendum I: Possible Mathematical Frame Work - the Energy Space Theory

We can formulate the variation of energy density at a higher order with a Taylor series development such as:

$$du = \partial_t u dt + \partial_t^2 u \frac{dt^2}{2} + o(dt^2) \quad (19)$$

$o$  is the Landau notation to omit higher order quantities. Note that at the first order  $\frac{du}{dt} = \partial_t u$ . Let us consider a mathematical frame work from [23]. The higher order orders term are based on the assumptions that the EM waves inside the skin layer of the copper end plate are functions in the Schwartz space  $\mathbf{S}^-(\mathbb{R}^2)$  ( $\mathbf{S}^-(\mathbb{R}^3)$  in 2D, in  $\mathbf{S}^-(\mathbb{R}^4)$  3D considering also the time variable - see [23]). In addition, they are finite energy function (i.e. following [23] and [24],  $L(E(x_0, y_0, z_0, T)) < \infty$  at some given point in the skin layer defined by the coordinates  $x_0, y_0, z_0$ ). Fortunately, these EM waves are evanescent waves [14]. In the last section of [23], it is shown why these waves can be function of the Schwartz space  $\mathbf{S}^-(\mathbb{R}^2)$  ( $\mathbf{S}^-(\mathbb{R}^3)$  or  $\mathbf{S}^-(\mathbb{R}^4)$  respectively). Now, using the **Lemma 1** (e.g. [23]) and the model based on the energy space in [24], let us introduce the subspace  $\mathbf{N}^i$  ( $i$  in  $\mathbb{Z}^+$ ) defined as

$$\begin{aligned} \mathbf{N}^i &= \{g \in \mathbf{S}^-(\mathbb{R}^3) \mid g = \partial_t^i (f^n(x_0, z_0, t)) \\ &= \alpha_n (\partial_t^{i-1} f^{n-2}(x_0, z_0, t) (\Psi_1^+(f(x_0, z_0, t)))) \\ , f &\in \mathbf{S}^-(\mathbb{R}^3), n \in \mathbb{Z}^+ - \{0\}, \alpha_n \in \mathbb{R}, z_0 \in [0, L], x_0 \in [0, a] \} \end{aligned} \quad (20)$$

With the definition of the family of energy operator  $(\Psi_k^+(\cdot))_{k \in \mathbb{Z}}$  from [23]. Here  $f$  is either the electric or magnetic field. In [24], the energy subspace is at the basis of the multiplicity of the solutions (e.g., **Theorem 2**, [24]). If  $g$  is a general solution of some linear PDEs, then  $f^n$  can be identified as a special form of the solution (conditionally to its existence).

Now considering the wave equation, the electric field and magnetic field are solutions and belong to the subspace  $\mathbf{N}^0$  and associated with the variation of energy density  $\partial_t w$ . Furthermore, we can consider the solutions in  $\mathbf{N}^1$  associated with the variation of energy density  $\partial_t^2 w$ , which can be explained with the *multiplicity* of waves and solutions of the wave equation [24]. The solutions of interest in  $\mathbf{N}^1$  are for the electric field  $g = \partial_t E$  and the magnetic field  $g = \partial_t B$ .

Another way to see the contribution of the functions in  $\mathbf{N}^1$ , is [24] with the Taylor Series development

of the energy of (for example) the electric field on a nominated position in space  $r_0$  and in an increment of time  $dt$ :

$$\begin{aligned}
L(E(r_0, T)) &= \int_0^T (R(r_0, u))^2 du < \infty \\
L(E(r_0, T + dt)) &= L(E(r_0, T)) + \sum_{k=0}^{\infty} \partial_t^k (E^2(r_0, T)) \frac{(dt)^k}{k!} < \infty \\
dL(E(r_0, T + dt)) &= \sum_{k=0}^{\infty} \partial_t^k (E^2(r_0, T)) \frac{(dt)^k}{k!} \\
dL(E(r_0, T + dt)) &= E^2(r_0, T)dt + \sum_{k=1}^{\infty} \partial_t^{k-1} (\Psi_1^{+,t}(E)(r_0, T)) \frac{(dt)^{k+1}}{k+1!} \\
dL(E(r_0, T + dt)) &\simeq E^2(r_0, T)dt + \Psi_1^{+,t}(E)(r_0, T) \frac{dt^2}{2} + \partial_t \Psi_1^{+,t}(E)(r_0, T) \frac{dt^3}{6}
\end{aligned} \tag{21}$$

Finally one can write the relationship with the energy density following (19) and the previous Taylor series development for the electric and magnetic field:

$$\begin{aligned}
0.5(\epsilon_0 \frac{dL(E(r_0, T + dt))}{dt} + \frac{1}{\mu_0} \frac{dL(B(r_0, T + dt))}{dt}) &= 0.5(\epsilon_0 E^2(r_0, T) \\
+ \frac{1}{\mu_0} B^2(r_0, T)) + \partial_t w \frac{dt}{2} + \partial_t^2 w \frac{dt^2}{6} + o(dt^2)
\end{aligned} \tag{22}$$

Therefore, taking into account the second order term of the energy density  $\partial_t^2 w$  means that additional solutions of the type  $\partial_t E$  and  $\partial_t B$  should also be considered in the EM modeling. That is an application of **Theorem 2** and the multiplicity/duplication theory in [24].

## ADDENDUM II: CONSEQUENCES IN TERMS OF EM THEORY

To recall Appendix I, the EM field is now including  $(\vec{E}, \delta\vec{E})$  and  $(\vec{B}, \delta\vec{B})$ , contribution of the subspaces  $\mathbf{N}^0$  and  $\mathbf{N}^1$  respectively. We call the total EM field  $\vec{E}_{tot}$  and  $\vec{B}_{tot}$  inside the copper plate (skin layer) with associated permittivity  $\epsilon_r$  and permeability  $\mu_r$ . They are solutions of the Maxwell equations:

$$\left. \begin{aligned}
div \vec{E}_{tot} &= \frac{\rho_{tot}}{\epsilon_r}, \\
curl \vec{E}_{tot} &= -\partial_t \vec{B}_{tot}, \\
div \vec{B}_{tot} &= 0, \\
curl \vec{B}_{tot} &= \mu_r \epsilon_r \partial_t \vec{E}_{tot} + \mu_r \vec{j},
\end{aligned} \right\}$$

with the principle of charge conservation:

$$\partial_t \rho_{tot} + div \vec{j} = 0 \tag{23}$$

Now, the variation of energy density (19) together with the equation of charge conservation is formulated such as:

$$\frac{dw}{dt} + div \vec{P}_{tot} = \vec{j} \cdot \vec{E}_{tot} \tag{24}$$

$\vec{P}_{tot} = \frac{\vec{E}_{tot} \times \vec{B}_{tot}}{\mu_r}$  is the Poynting vector. Now, writing  $\vec{E}_{tot} = \vec{E} + \delta\vec{E}$ ,  $\vec{B}_{tot} = \vec{B} + \delta\vec{B}$  and  $\delta$  is the first derivative in time ( $\partial_t$ ) (i.e. solutions in  $\mathbf{N}^1$  - see Addendum I), then following [14]

$$(\vec{E} + \partial_t \vec{E}) \cdot \vec{j} = (\vec{E} + \partial_t \vec{E}) \cdot \left[ \frac{1}{\mu_r} curl (\vec{B} + \partial_t \vec{B}) - \epsilon_r \partial_t (\vec{E} + \partial_t \vec{E}) \right] \tag{25}$$

using the equalities  $\text{div} (\vec{E} \times \vec{B}) = \vec{B} \cdot \text{curl} \vec{E} - \vec{E} \cdot \text{curl} \vec{B}$  and the Maxwell equation  $\text{curl} \vec{E} = -\partial_t \vec{B}$ ,  $\text{curl} \partial_t \vec{E} = -\partial_t^2 \vec{B}$  the previous equation reduces to:

$$\begin{aligned} & \vec{E} \cdot \vec{j} + \text{div} \left( \frac{\vec{E} \times \vec{B}}{\mu_r} \right) + \partial_t w + \\ & \partial_t \vec{E} \cdot \vec{j} + \text{div} \left( \frac{\partial_t \vec{E} \times \partial_t \vec{B}}{\mu_r} \right) + \partial_t^2 w + \\ & \text{div} \left( \frac{\partial_t \vec{E} \times \vec{B}}{\mu_r} \right) + \text{div} \left( \frac{\vec{E} \times \partial_t \vec{B}}{\mu_r} \right) + \frac{\partial \vec{B} \cdot \partial \vec{B}}{\mu_r} + \epsilon_r \partial_t \vec{E} \cdot \partial_t \vec{E} = 0 \end{aligned} \quad (26)$$

We can separate in three groups,

$$\left. \begin{aligned} \partial_t w + \text{div} \left( \frac{\vec{E} \times \vec{B}}{\mu_r} \right) &= -\vec{j} \cdot \vec{E} \\ \partial_t^2 w + \text{div} \left( \frac{\partial_t \vec{E} \times \vec{B}}{\mu_r} \right) + \text{div} \left( \frac{\vec{E} \times \partial_t \vec{B}}{\mu_r} \right) &= -\vec{j} \cdot \partial_t \vec{E} \\ \text{div} \left( \frac{\partial_t \vec{E} \times \partial_t \vec{B}}{\mu_r} \right) &= -\frac{\partial_t \vec{B} \cdot \partial_t \vec{B}}{\mu_r} - \epsilon_r \partial_t \vec{E} \cdot \partial_t \vec{E} \end{aligned} \right\}$$

The Poynting vector is defined as  $\vec{P} = \frac{\vec{E} \times \vec{B}}{\mu_r}$  and its derivative  $\partial_t \vec{P} = \frac{\partial_t \vec{E} \times \vec{B}}{\mu_r} + \frac{\vec{E} \times \partial_t \vec{B}}{\mu_r}$ . Thus, the second order term of the energy density is the contribution of the EM field generated by  $\partial_t \vec{E}$  and  $\partial_t \vec{B}$  is:

$$\left. \begin{aligned} \partial_t w + \text{div} \vec{P} &= -\vec{j} \cdot \vec{E} \\ \partial_t^2 w + \text{div} (\partial_t \vec{P}) &= -\vec{j} \cdot \partial_t \vec{E} \\ \text{div} \left( \frac{\partial_t \vec{E} \times \partial_t \vec{B}}{\mu_r} \right) &= -\frac{\partial_t \vec{B} \cdot \partial_t \vec{B}}{\mu_r} - \epsilon_0 \partial_t \vec{E} \cdot \partial_t \vec{E} \end{aligned} \right\}$$

The last line is the contribution from only the fields  $\partial_t \vec{E}$  and  $\partial_t \vec{B}$ .

Finally, the creation of the wave defined by the EM field  $(\partial_t \vec{E}, \partial_t \vec{B})$  means that some material properties may allow to create two type of EM waves namely  $(\vec{E}, \vec{B})$  and  $(\partial_t \vec{E}, \partial_t \vec{B})$ .

### ADDENDUM III: DERIVATION OF THE WOODWARD EFFECT USING THE ELECTROMAGNETIC ENERGY DENSITY

#### Assumptions with the energy momentum relationship

When the Woodward effect was established in [4], the authors implicitly assumed the rest mass of the piezoelectric material via the famous Einstein's relation in special relativity  $\mathcal{E} = mc^2$  ( $\mathcal{E}$  the rest energy associated with the rest mass  $m$ ) and its variation via electrostrictive effect.

Here, the system is the frustum. The rest mass is all the particles within it at the time of the capacitor is discharged. It excludes the photons considered with a null mass. Thus, the main assumption is that the EM excitation on the end plates creates electric charges (i.e. electrons) which makes the rest mass varying with time. This assumption is the same as the mass variation of a capacitor between the charge and discharge times [25]. It allows us to state the variation of rest energy such as:

$$\begin{aligned} \Delta \mathcal{E} &= \mathcal{E}(t + dt) - \mathcal{E}(t) \\ &= (m(t + dt) - m(t))c^2 \\ &= \Delta m c^2 \end{aligned} \quad (27)$$

Finally, the variation of rest energy  $\Delta \mathcal{E}$  is assumed to be equal to the variation of EM energy density ( $\Delta u_{EM}$ ) resulting from the charges within the skin depth of the copper walls. We also cannot forget the electrostrictive effect ( $\Delta u_{El}$ ) when inserting HDPE disk(s) inside the frustum, but we consider that  $\Delta u_{EM} \gg \Delta u_{El}$ .

Note that at the particle level, the rest mass should satisfy the energy momentum relationship for a free body in special relativity [26]:

$$\begin{aligned} u_e^2 &= (pc)^2 + (m_e c^2)^2 \\ p &= v \frac{u_e}{c^2} \end{aligned} \quad (28)$$

with  $p$  the momentum and  $m_e$  the rest mass of the particle associated with the total energy  $u_e$ . The particle is accelerated via the Lorentz force applied to the whole cavity with obviously  $v \ll c$ . Thus, we have also the relationship  $p^2 < (u_e/c)^2$ .

### Woodward effect

From [4], one can write the mass variation per unit of volume

$$dm = \frac{\delta m}{V}$$

$$dm = \frac{1}{4\pi G} \left[ \frac{1}{m} \partial_t^2 m - \frac{1}{m^2} (\partial_t m)^2 \right] \quad (29)$$

If we define the mass density such as  $\rho = m/V$ , then

$$\delta\rho = \frac{\delta m}{V}$$

$$\delta\rho = \frac{1}{4\pi G} \left[ \frac{1}{\rho} \partial_t^2 \rho - \frac{1}{\rho^2} (\partial_t \rho)^2 \right] \quad (30)$$

Let us define the the rest energy  $\mathcal{E} = \rho c^2$ , then

$$\delta\rho = \frac{1}{4\pi G} \left[ \frac{1}{\rho c^2} \partial_t^2 \mathcal{E} - \frac{1}{(\rho c^2)^2} (\partial_t \mathcal{E})^2 \right]$$

$$\delta\rho = \frac{1}{4\pi G} \left[ \frac{1}{\mathcal{E}} \partial_t^2 \mathcal{E} - \frac{1}{(\mathcal{E})^2} (\partial_t \mathcal{E})^2 \right] \quad (31)$$

Now, with the assumption that the variation in time of the rest energy is equal to the variation of EM energy density  $u$

$$\delta\rho = \frac{1}{4\pi G} \left[ \frac{1}{\mathcal{E}} \partial_t^2 u - \frac{1}{(\mathcal{E})^2} (\partial_t u)^2 \right] \quad (32)$$

The EM energy density  $u$  follows the general definition of the sum of energy density from the electric ( $u_E$ ) and magnetic ( $u_B$ ) fields [14].

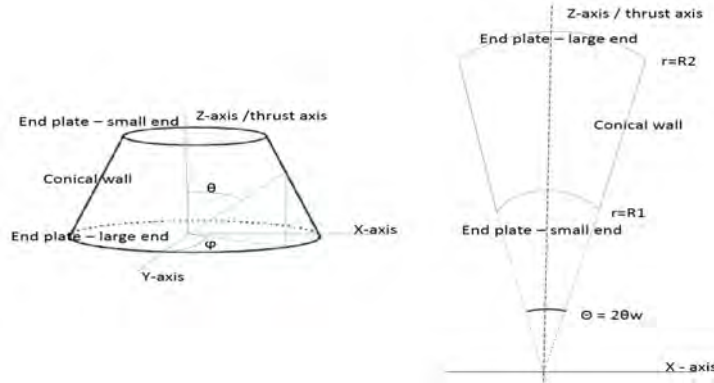


FIG. 1: Drawing of the EM Drive cavity

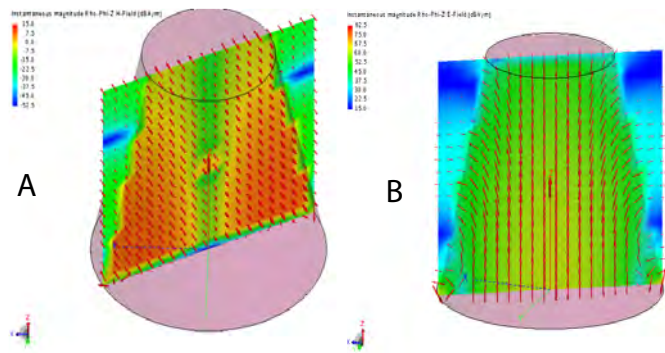


FIG. 2: Simulations of the EM field inside the frustum in TM<sub>010</sub> mode: (A) magnetic field, (B) electric field

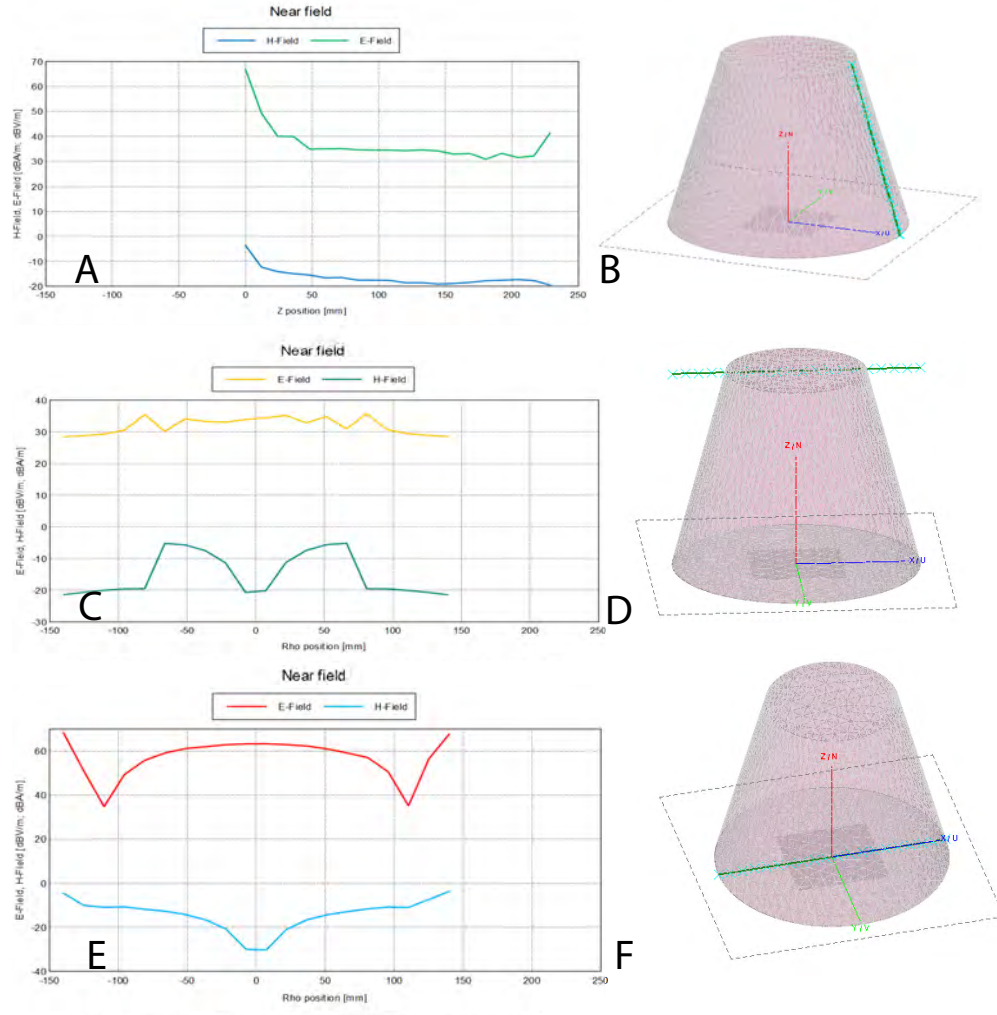


FIG. 3: Estimation of surface currents (A,B) conical wall, (C,D) small end, (E,F) large end. Note that rho is the x-axis (blue line), z-axis is the red line

## REFERENCES

- [1] R. Shawyer, *The EM Drive a New Satellite Propulsion Technology*, in Proc. of the 2nd Conference on Disruptive Technology in Space Activities, 2010.
- [2] R. Shawyer, *Second generation EmDrive propulsion applied to SSTO launcher and interstellar probe*, Acta Astronautica, p. 166-174.  
Doi:<http://dx.doi.org/10.1016/j.actaastro.2015.07.002>
- [3] H. Fearn, A. Zachar, J. F. Woodward and K. Wanser, *Theory of a Mach Effect Thruster*, in Proc. of the AIAA Joint Propulsion Conference, Tech. Session: Nuclear and Future Flight Propulsion, <http://arc.aiaa.org/doi/abs/10.2514/6.2014-3821>.
- [4] J. F. Woodward, *Life Imitating Art: Flux Capacitors, Mach Effects, and Our Future in Spacetime*, AIP Conference Proceedings. Space Technology Applications International Forum (STAIF 2004), Albuquerque, New Mexico. American Institute of Physics. p. 11271137, 2004. Doi: 10.1063/1.1649682.
- [5] D.A. Brady, H.G. White, P. March, J.T. Lawrence, and F.J. Davies, *Anomalous Thrust Production from an RF Test Device Measured on a Low-Thrust Torsion Pendulum*, AIAA 2014-4029, 2014.
- [6] H. White, P. March, J. Lawrence, J. Vera, A. Sylvester, D. Brady, P. Bailey, *Measurement of Impulsive Thrust from Closed Radio Frequency Cavity in Vacuum*, AIAA Journal of Propulsion and Power, December, 2016.
- [7] M. Tajmar, and G. Fiedler, *Direct Thrust Measurements of an EM Drive and Evaluation of Possible Side-Effects*, in Proc. of the 51st AIAA/SAE/ASEE Joint Propulsion Conference, AIAA 2015-4083. Doi: 10.2514/6.2015-4083
- [8] J.F. Woodward, *Making Starships and Stargates*, Springer-Verlag New York, 2013. Doi: 10.1007/978-1-4614-5623-0
- [9] M. E. McCulloch, *Can the Emdrive Be Explained by Quantised Inertia ?*, Progress in Physics, vol. 11, 2015.
- [10] P. Grahn, A. Annala, E. Kolehmainen, *On the Exhaust of Electromagnetic Drive*, AIP Advances, vol. 6 (6), 2016. Doi: 10.1063/1.4953807
- [11] T. J. Desiato, *An Engineering Model of Quantum Gravity*, September, 2016.
- [12] J.F. Woodward, *Gravity, Inertia, and Quantum Vacuum Zero Point Fields*, Foundations of Physics, 31 (5), p. 819835, 2001. Doi: 10.1023/A:1017500513005
- [13] D. W. Sciama, *On the Origin of Inertia*, Monthly Notices of the Royal Astronomical Society, vol. 113 (1), p. 34-42, 1953. Doi: 10.1093/mnras/113.1.34
- [14] R. Petit, *Ondes Electromagnetiques en radioelectricite et en optique*, 2nd Edition, Masson, 1993.
- [15] A. E. Fitzgerald, C. (Jr) Kingsley, S. D. Umans, *Electric Machinery*, 4th ed., Mc-Graw-Hill, Inc. p. 20, 1983. (ISBN 0-07-021145-0)
- [16] G.G. Raju, *Dielectrics in Electric Fields*, CRC Press, 2003. (ISBN:9780824708641).
- [17] MIT Web lecture, *Resonant Cavities and Waveguides*,  
<http://web.mit.edu/22.09/ClassHandouts/ChargedParticleAccel/CHAP12.PDF>
- [18] J. Rodal, *Resonant Cavity Space Propulsion*  
<https://forum.nasaspaceflight.com/index.php?topic=39214.msg1546438#msg1546438>
- [19] G. Egan, *Resonant Modes of a Conical Cavity*.  
<http://gregegan.customer.netspace.net.au/SCIENCE/Cavity/Cavity.html>
- [20] David R. Lide, *CRC Handbook of Chemistry and Physics*, CRC Press Inc, 2009, 90e Ed., 2804.(ISBN 978-1-420-09084-0)

- [21 ] D. H. Staelin, *Electromagnetics and Applications*, Department of Electrical Engineering and Computer Science, Massachusetts Institute of Technology, Cambridge MA. Available at: <https://ocw.mit.edu/courses/> or google  
MIT6\_013S09\_notes.pdf
- [22 ] F. J. Davies, *Copper Frustum Modes*, Personal Communication, NASA Johnson Space Center ,  
NASA/JSC/EP5.
- [23 ] J.P. Montillet, *The Generalization of the Decomposition of Functions by Energy Operators (Part II) and Some Applications*, Acta Applicandae Mathematicae. doi: 10.1007/s10440-014-9978-9, also available at: <http://arxiv.org/abs/1308.0874>.
- [24 ] J.P. Montillet, *Multiplicity of Solutions for Linear Partial Differential Equations Using (Generalized) Energy Operators*, available in: <http://arxiv.org/pdf/1509.02603v1.pdf>
- [25 ] E. B. Porcelli, V. S. Filho, *On the Anomalous Weight Losses of High Voltage Symmetrical Capacitors*, ArXiv. doi: 10.4006/0836-1398-29.1.002
- [26 ] C. Möller, *The Theory of Relativity*, 2nd ed., Delhi: Oxford University Press. p. 220, 1952. ISBN 0-19-560539-X.
- [27 ] P. March, *Examination of Eagleworks (EW) Labs Copper Frustums TM010 Resonant Mode Thrust Production with and without Dielectric Discs in the frustum at 90W RF*, 2016.
- [28 ] FEKO, <https://www.feko.info/references/publications-citing-feko>